Comprehensive Flood Impact Assessment for Bridge Infrastructure Using Integrated AHP and Fuzzy AHP Analysis: Iowa Case Study

Ege Duran[1,2], Jerry Mount[1], Ibrahim Demir[3,4]

[1] IIHR Hydroscience and Engineering, University of Iowa, Iowa City, IA, USA
[2] Civil and Environmental Engineering, University of Iowa, Iowa City, IA, USA
[3] River-Coastal Science and Engineering, Tulane University, New Orleans, LA, USA
[4] ByWater Institute, Tulane University, New Orleans, LA, USA
*Corresponding Author: ege-duran@uiowa.edu

Abstract

Flooding poses a significant threat to transportation infrastructure like bridges and culverts in regions like Iowa, where infrastructure deficiencies, unpredictable climate patterns, and geographic factors all contribute to vulnerability. This study evaluates the susceptibility of over 24,000 bridges in Iowa to flood-induced damage by considering both the likelihood of flooding and its potential negative impacts on bridge functionality, using the Analytic Hierarchy Process (AHP) and Fuzzy AHP methods. By combining bridge inventory datasets with historical flood data, this study assesses flood risks across multiple flood scenarios (50, 100, and 500 years return period). Factors such as bridge age, condition, traffic volume, detour lengths, and flood likelihood were used to calculate the impact indices for each bridge. Two distinct impact index sets were computed and visualized across the state at individual locations, county scales, and through a Kernel-based heatmap analysis where the population data was incorporated as an additional layer to provide a broader perspective on the potential societal impacts. The results indicate areas where a large portion of the bridge network is at risk of flooding, potentially leading to major disruptions and impacts on society. This research provides insights into the weaknesses in Iowa's bridge network and contributes to understanding how transportation infrastructure is impacted by flooding.

Keywords: Flood Impact, Risk Assessment, Bridge Vulnerability, Transportation Infrastructure

1. Introduction

Floods are recurring disasters that pose severe socio-economic challenges, causing loss of life and damage to property worldwide (Adhikari et al., 2010). These disasters arise from multiple factors, including hydrological variations, rainfall distribution, land cover changes, and soil moisture levels, which impact flood severity and frequency (Lebbe et al., 2014; Seo et al., 2019). In addition to its immediate physical damage, flooding has long-term consequences for ecosystems and communities (Crawford et al., 2022). Given the increasing unpredictability of climate patterns, effective flood risk management has become a priority in land-use planning worldwide (Mitchell, 2005; Tanir et al., 2024).

Flooding poses severe social and economic risk, resulting in extensive disturbances and significant financial and ecological damages (Alabbad et al., 2023). Floods impose substantial economic costs and are among the most financially disruptive natural disasters in the United States (Highfield and Brody, 2017). With increasing frequency and severity of flooding due to population growth and urban development (Zhang et al., 2018; Sadler et al., 2017), the estimated annual flood damage costs have risen sharply, from $6 billion in 2005 to projections exceeding $60 billion by 2050 (Rentschler et al., 2022). Furthermore, floods have a significant impact on transportation infrastructure, resulting in the closure of roads and bridges that disrupt daily commuting, supply chains, and emergency response efforts (Alabbad & Demir, 2024). These closures have both direct and indirect effects on individuals who do not work from home, resulting in psychological distress, as well as reductions in work hours and Gross Domestic Product (GDP) (Botzen et al., 2019).

Iowa's flood risk is underscored by its numerous historical flooding events, particularly the most significant one in 2008, which was one of the costliest disasters in the United States (USGS, 2010). The Midwest region of the United States, particularly Iowa, is among the most flood-prone areas, experiencing frequent extreme weather events and riverine flooding (Sit et al., 2021). This vulnerability is largely due to Iowa's landscape, shaped by major waterways such as the Mississippi River to the east and the Missouri River to the west, which contribute to extensive flooding events (Li et al., 2023a).

It is essential to understand the flood risk on critical infrastructure to ensure the dependability and resilience of essential services during disasters (Cikmaz et al., 2024). Although certain disruptions, such as temporary closures, may be inevitable, the identification of systemic vulnerabilities assists in the improvement of long-term mitigation and response strategies (Yildirim et al., 2023). Among the critical infrastructure networks, transportation systems are particularly vulnerable to flooding due to their dependency on bridges and roads, which are often inundated during severe flood events (Alabbad et al., 2024). Bridges, in particular, are essential elements of transportation networks, supporting economic activity, emergency response operations, and access to key services such as hospitals and schools (Pregnolato et al., 2018), and their importance is further emphasized in the event of disruptions (Wright et al., 2012). Due to their critical role in transportation, crossing structures like bridges and tunnels cannot be easily removed or modified such as berms or other floodplain infrastructure (Seigel, 2021).

While roads may have alternative routes during floods, bridges often provide essential connections over rivers or valleys that cannot be bypassed, leading to severe traffic disruptions. Given their role in ensuring the mobility of both people and goods, understanding the flood risk to bridge infrastructure is critical for strengthening disaster resilience and ensuring continuity in essential services (Garlock et al., 2012). For instance, authorities can prepare for an imminent flooding season and establish emergency routes by identifying bridges that are susceptible to flooding (Ciftcioglu and Naser, 2024).

Despite extensive research on flood mitigation strategies, infrastructure vulnerability assessments (Cikmaz et al., 2022), and damage cost estimation models (Yildirim et al., 2022), there remains a notable gap in flood impact studies focusing on bridges. Multiple criteria decision-making (MCDM) methods are frequently implemented in impact and risk assessments (Rincón et al., 2018; Xu et al., 2019). These methods involve selecting potential alternatives in advance, after which decision-makers rank them based on an evaluation of multiple criteria (Sadiq and Tesfamariam, 2009). While MCDM methods have been widely applied in flood risk assessments (Papaioannou et al., 2015; Khosravi et al., 2019), few studies have examined flood-related bridge disruptions with a structured decision-making approach.

Recent studies have also introduced fuzzy logic-based methodologies, which improve risk assessments by incorporating uncertainty and imprecise expert judgments (Ziegelaar and Kuleshov, 2022). While some studies focus exclusively on fuzzy approaches due to their ability to handle uncertainty (Engel and Last, 2007; Liu and Tsai, 2012), AHP remains valuable for its structured, hierarchical decision-making framework (Vaidya and Kumar, 2006). Combining AHP and Fuzzy AHP provides a more comprehensive evaluation of flood risks, allowing for both structured prioritization and uncertainty modeling (Das, 2010), which is a key driver for this research.

Studies like Shariati et al. (2023) have applied AHP and Fuzzy AHP methods in flood hazard assessments. This study applies these methods to bridge flood risk assessments in Iowa. By integrating bridge inventory data, elevation model and flood hazard maps, we evaluate the impact of bridge closures across multiple return periods (50, 100, and 500 years). This approach considers structural and functional parameters, including bridge condition, traffic volume, detour lengths, and inundation status, to generate impact index. Additionally, we utilize spatial visualization techniques, including kernel density analysis, to highlight critical hotspots. The findings will provide transportation planners and policymakers with actionable insights, guiding flood mitigation efforts and improving infrastructure resilience in the face of increasing flood threats.

The remainder of our study is structured into three main parts: methodology, results and discussion, and conclusion. The methodology part details the data preparation process, bridge inundation analysis, parameter selection, and the application of AHP and Fuzzy AHP for vulnerability assessment. In the results and discussion part, we present our findings on bridge vulnerability at both the county scale and individual bridge locations, compare AHP and Fuzzy AHP outputs, and analyze their implications for flood risk management. Finally, the conclusion

section summarizes key insights, highlights their significance for infrastructure resilience, and suggests directions for future research to enhance flood risk assessments.

2. Methodology

This section explains the methodical process utilized to evaluate bridge susceptibility to flooding and subsequent impact on the transportation network. The methodology includes data preparation, bridge inundation evaluation, and the application of the Analytic Hierarchy Process (AHP) and Fuzzy AHP to assess and quantify the factors influencing bridge flood impact. Each step in the analysis process is detailed to ensure transparency, repeatability, and validation to support future studies and enable implementation of the approach.

2.1. Data Preparation

This study utilized National Bridge Inventory (NBI) data to gather detailed bridge specifications such as location, structure number, owner, type, service, and construction year. Bridge overtopping during flood events is evaluated using flood inundation model depth raster created by the Iowa Flood Center and Iowa Department of Natural Resources. These datasets, with a 1-meter resolution, visualize the extent and depth of flooding for multiple return periods (50-year, 100-year, and 500-year) and used in evaluation studies (Li et al., 2023b), based on topographical and hydraulic data (Gilles et al., 2012). The census block population is included as a weight in the Kernel Density Estimation process, emphasizing how the population contributes to the overall bridge inundation impact, providing a more comprehensive understanding of the affected areas and demographics.

Iowa has over 24,000 bridges, with 93% of them spanning waterways, making them particularly susceptible to flooding and presenting significant transportation challenges. This vulnerability necessitates careful monitoring and maintenance to ensure the safety and longevity of these structures. To evaluate Iowa's bridge conditions within the broader context of national trends, we used annual data from the Federal Highway Administration (FHWA), covering the years from 1992 to 2024. This analysis enabled us to evaluate Iowa's bridge inventory compared to other states, focusing on the total number of bridges, number of bridges in poor condition, and percentage of poor bridges within the state. Figure 1 ranks the data, ensuring internal consistency and avoiding potential distortions from changes in evaluation standards or regulations over the years. This approach provides an internally consistent and accurate comparison of Iowa's progress relative to other states.

Iowa's ranking trends over time are illustrated in the graph above, which also shows the state's position about the total number of bridges and bridge conditions. Iowa still has one of the largest bridge inventories among states (top 10), with its overall bridge number fluctuating between 5th and 8th place, staying relatively stable over the years. Despite this stability, in terms of poor bridge numbers, Iowa first entered the top 3 in 1998 and moved into the top 2 by 2008. It ranked 1st in 2014 and maintained that position until 2023. Iowa's change in ranking has been more dramatic in terms of its "poor bridge score" percentage rank compared to the other states. In 1992, Iowa ranked

12th in the percentage of poor-condition bridges, rising to the top three by 2008, where it has remained since. While Iowa's actual number and percentage of poor bridges decreased over time, its relative standing compared to other states also declined. This suggests that while Iowa is making progress in reducing the number of poor bridges, its efforts are not advancing as quickly as those of other states, resulting in a decline in relative performance.

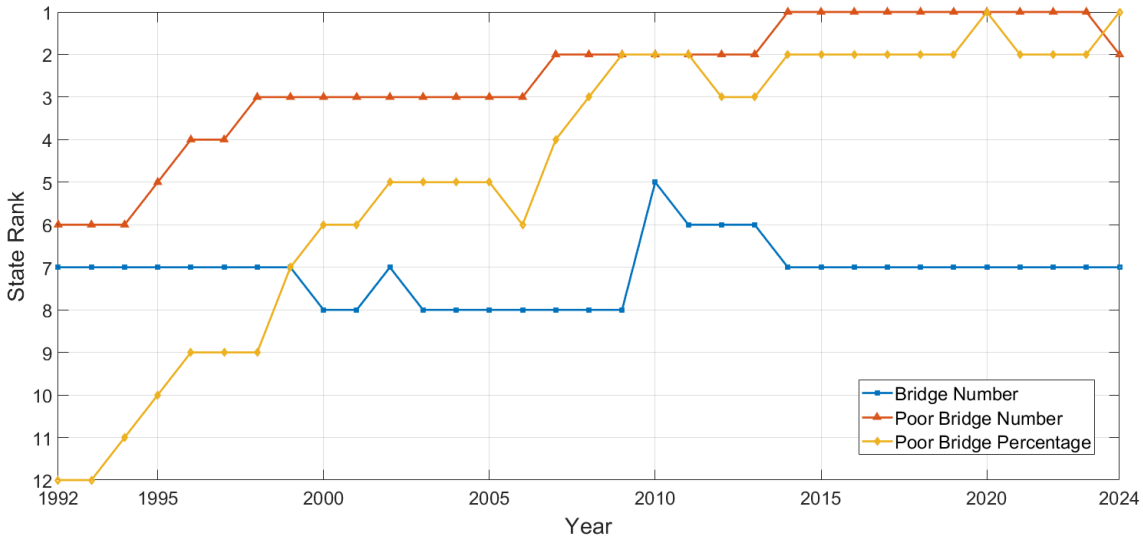

Figure 1. Iowa state bridge inventory ranking among the US over the years.

2.2. Bridge Inundation Computation

This study utilizes bridge inventory data, flood depth models, and Iowa State's bare-earth Digital Elevation Model (DEM) to analyze three flood scenarios using GIS software. This process involves analyzing the spatial distribution of bridges across counties, evaluating traffic networks, and examining key statistics such as bridge condition and construction year. These factors are then used to assess the criticality of each bridge in the context of flood risk. The study also incorporates three-dimensional analysis by including bare earth elevation data, which adds depth to the analysis of flood risks and bridge design. Bridge deck heights are determined using lidar (Light Detection and Ranging) data from GeoInformatics Training Research Education and Extension (GeoTree), which enables a more accurate assessment of potential flooding and overtopping risks. Floodwater covering the bridge surface renders it unusable and closed, making it functionally equivalent to a collapsed bridge (Duran et al., 2025).

To determine the values being compared in the flood impact analysis, the centroid of each bridge in 2D is identified and used to extract the corresponding elevation values from the DEM and LIDAR data. The bridge deck height (HD) is then determined by selecting the closest LIDAR data point to the bridge centroid, to capture the maximum flood depth and deck height, ensuring accurate predictions of bridge inundation and more reliable calculations. The bare-earth elevation (HBE) is derived from the DEM, while the Hydrologic Unit Code (HUC8) watershed flood depth (HF) is obtained from Iowa Geospatial Data Clearinghouse (IGDC). These parameters are utilized

in Equation 1 to calculate the flood depth relative to the bridge deck height and determine whether the bridge is inundated.

$$\begin{aligned} \text{Fi} &= \text{HD} - \text{HBE} + \text{HF}\,;\ \text{If Fi} > 0, \text{bridge is inundated;} \\ &\quad \text{if Fi} < 0, \text{bridge is not inundated} \end{aligned} \qquad \text{Eq. 1}$$

2.3. Correlation Analysis for Parameter Selection

In this analysis, we examine the relationships between key bridge parameters that affect their vulnerability to flooding. A common approach is to convert categorical variables into numerical values and then calculate the correlation (Ciftcioglu and Naser, 2024). A quantitative evaluation of the complex interactions among bridge parameters is made possible by the Pearson correlation analysis. This method is ideal for normalized datasets, typically free from outliers, and provides a quantitative measure of the strength and direction of relationships between variables (Duran and Demir, 2024). The Pearson correlation coefficient (r) is calculated for each pair of variables to quantify the strength and direction of their relationships below in Equation 2.

$$r = \frac{\sum(x_i - \bar{x})(y_i - \bar{y})}{\sqrt{\sum(x_i - \bar{x})^2 \sum(y_i - \bar{y})^2}} \qquad \text{Eq. 2}$$

In this equation, r is the Pearson correlation coefficient, x_i and y_i are two variables being compared, and $\bar{x}$ and $\bar{y}$ are their mean values. The correlation coefficient can differ between -1 and 1, with a positive value indicating a direct correlation and a negative value suggesting an inverse relationship. An absolute value of Pearson correlation coefficient greater than 0.7 is considered a strong correlation (Kuckartz et al., 2013).

Table 1. Correlation Matrix for Impact Index Parameter Selection.

	50 year	**100 year**	**500 year**	**Age**	**Condition**	**Waterway**	**Length**	**ADT**	**Detour**
50 year	1.00	0.84	0.68	0.03	-0.07	-0.09	-0.04	-0.07	0.03
100 year	0.84	1.00	0.81	0.02	-0.08	-0.10	-0.04	-0.06	0.04
500 year	0.68	0.81	1.00	0.02	-0.08	-0.09	-0.06	-0.08	0.04
Age	0.03	0.02	0.02	1.00	-0.63	-0.45	-0.07	-0.06	0.01
Condition	-0.07	-0.08	-0.08	-0.63	1.00	0.48	0.08	0.10	-0.04
Waterway	-0.09	-0.10	-0.09	-0.45	0.48	1.00	0.13	0.04	-0.06
Length	-0.04	-0.04	-0.06	-0.07	0.08	0.13	1.00	0.29	-4x10-5
ADT	-0.07	-0.06	-0.08	-0.06	0.10	0.04	0.29	1.00	-0.06
Detour	0.03	0.04	0.04	0.01	-0.04	-0.06	-4x10-5	-0.06	1.00

Table 1 presents the correlation matrix, highlighting relationships between key variables over time. Notably, bridge length shows a weak correlation with other parameters, while age-condition

and age-waterway evaluation pairs exhibit strong negative correlations, meaning that as one increases, the other decreases. Additionally, bridge condition and waterway evaluation are strongly correlated. Given these relationships, bridge condition and age were selected as structural parameters due to their inverse correlations with waterway evaluation, as well as their ability to represent each other.

Annual daily traffic and detour length are used as traffic parameters, as they help assess the disruption caused by bridge closures. The average daily traffic can be determined by calculating the total number of vehicles passing through a specific location over a period of 24 hours each day for 365 days. This total count is then divided by 365 to obtain the average daily traffic value (Huntsinger, 2022). The detour length is computed by determining the additional distance a vehicle must travel along a designated detour route to reach its destination, in comparison to the original, shortest route that would have been taken if the bridge were open (US DOT, 1995). Since we are examining the impacts of the closures, using both average daily traffic and detour parameters provides a more comprehensive approach.

In our study, we normalized the flood closure parameters by creating an ordinal code that represents multiple values. Instead of using three different flood scenarios with two options (open or closed), we combined these into one parameter with four options, based on the number of closure cases for each bridge. If a bridge is closed in all three scenarios, it is assigned a value of 3. If it is only closed in the 100- and 500-year scenarios, it receives a value of 2. Conversely, if the bridge remains open in all scenarios, it is assigned a value of 0, indicating that the closure analysis does not apply to that bridge.

2.4. Analytic Hierarchy Process

We utilized the Analytic Hierarchy Process to assess bridges' susceptibility to flooding and obtain a better understanding of the relative importance of multiple variables. Flood risk assessment is a complex and multifaceted process that involves both quantitative and qualitative factors, many of which are highly uncertain (Yang et al, 2013). The Analytic Hierarchy Process breaks down a complex multi-criteria decision-making (MCDM) problem into a hierarchical structure, evaluates the relative significance of various decision criteria, compares alternatives based on each criterion, and establishes an overall priority and ranking for the decision options (Wang et al., 2008). Since not all factors play an equal role in the flooding issue, this technique helps assign appropriate weights to each factor based on its significance. (Doorga et al., 2008). The AHP is particularly focused on deviations from consistency, how they are measured, and how they depend on one another and on the groups of structural elements (Saaty, 1987). This section outlines the overall computational steps.

Determination of Risk Factors: The comparative matrix represents the relative importance of numerical values based on the AHP scale. The following expression is used for constructing a pairwise matrix:

$$A = \begin{pmatrix} a_{11} & \cdots & a_{1n} \\ \vdots & \ddots & \vdots \\ a_{n1} & \cdots & a_{nn} \end{pmatrix} \quad \text{Eq. 3}$$

Building the Ordinal Hierarchy: Our hierarchy emphasizes that closure is the most critical factor influencing flood risk assessment since it directly impacts bridge accessibility and traffic flow. Average Daily Traffic (ADT) and detour length are equally important, reflecting the criticality of traffic load and the closure effects of rerouting. On the other hand, condition and age are contributing as the structural integrity assessment because they are secondary to the immediate impacts of closure on disruptions. By prioritizing these parameters, our analysis addresses flood risk management and bridge safety more effectively.

Computing Pairwise Comparisons: We conducted pairwise comparisons between each pair of parameters at the same level in the hierarchy. We utilized a scale to express the relative preference of one criterion over another. This is a numerical scale from 1 to 9, as can be seen in Table 2, with 1 indicating equal importance and 9 indicating extremely greater importance.

Table 2. AHP and Fuzzy AHP Scales for Pairwise Comparison Matrix (Putra et al., 2018).

Interpretation	**AHP Scale**	**TFN Scale**	**Reciprocal TFN Scale**
Equally Important	1	(1, 1, 1)	(1, 1, 1)
Equal to Moderate	2	(0.5, 1, 1.5)	(0.67, 1, 2)
Moderately Important	3	(1, 1.5, 2)	(0.5, 0.67, 1)
Moderate to Important	4	(1.5, 2, 2.5)	(0.4, 0.5, 0.67)
Important	5	(2, 2.5, 3)	(0.33, 0.4, 0.5)
Important to High Important	6	(2.5, 3, 3.5)	(0.28, 0.33, 0.4)
High Important	7	(3, 3.5, 4)	(0.25, 0.28, 0.33)
High to Extreme Important	8	(3.5, 4, 4.5)	(0.22, 0.25, 0.28)
Extremely Important	9	(4, 4.5, 4.5)	(0.22, 0.22, 0.25)

Building Pairwise Comparison Matrices: We created matrices for each level in the hierarchy based on the pairwise comparisons provided previously. Then we used the values assigned in the comparisons to populate the matrices, as can be obtained from Table 3.

Table 3. Pairwise Comparison Matrix.

	Age	**Condition**	**ADT**	**Detour**	**Closure**
Age	1	0.5	0.33	0.33	0.2
Condition	2	1	0.5	0.5	0.25
ADT	3	2	1	1	0.33
Detour	3	2	1	1	0.33
Closure	5	4	3	3	1
SUM	14	9.5	5.83	5.83	2.12

AHP Weights of Each Parameter: After creating the pairwise matrix, the results are normalized using Equation 4 and Equation 5 to ensure that each parameter's weight is proportionally represented for further calculations.

$$b_{ij} = \frac{a_i}{\sum_{i=1}^{n} a_{ij}} \quad \text{Eq. 4}$$

$$A = \begin{pmatrix} b_{11} & b_{12} & \dots & b_{1m} \\ b_{21} & b_{22} & \dots & b_{2m} \\ b_{n1} & b_{n2} & \dots & b_{nm} \end{pmatrix} \quad \text{Eq. 5}$$

Calculating Relative Weights: To find the weight of each parameter, the average of each row is estimated in the normalized pairwise comparison matrix using Equation 6, where "n" represents the number of factors.

$$W_i = \frac{\sum_{i=1}^{n} b_{ij}}{n}; \text{ where } \sum_{i=1}^{n} W_i = 1 \quad \text{Eq. 6}$$

Checking for Consistency: The consistency ratio is calculated by comparing the consistency index to a random index. If the ratio is within an acceptable range (below 0.1), the comparisons are considered consistent (Saaty, 1987).

$$CR = \frac{\text{Consistency Index (CI)}}{\text{Random Index (RI)}} \quad \text{Eq. 7}$$

$$CI = \frac{\lambda_{max} - n}{n - 1} \quad \text{Eq. 8}$$

In Equation 8, λ_{max} is the largest Eigenvalue from the pairwise matrix, and n is the number of parameters (Malczewski, 1999). As can be seen in the table below, RI is random index and n is our dependent count, which is 5. The CR value is below 0.1, indicating that the data are nearly fully consistent and considered acceptable.

Table 4. Random Index (RI) (Saaty, 1980)

n	1	2	3	4	5	6	7	8	9
RI	0	0	0.58	0.90	1.12	1.24	1.32	1.41	1.45

Table 5. Consistency Index and Ratio

λ_{max}	5.057
Consistency Index (CI)	0.014
Consistency Ratio (CR)	0.013

One of the key advantages of the Analytic Hierarchy Process is its organized and systematic approach to decision-making. The development of consensus among decision-makers is also aided by this approach. However, there are drawbacks to AHP, including its sensitivity to shifts in criteria and judgments and the possibility of subjectivity in pairwise comparisons, which could introduce bias (Pourghasemi et al., 2012). Due to these issues, this study utilizes the Fuzzy AHP method to avoid the limitations of the traditional Analytic Hierarchy Process, building upon its framework.

2.5. Fuzzy Analytic Hierarchy Process

Flood risk evaluation is an inherently complex and multidimensional process that involves both quantitative and qualitative factors, many of which may carry a degree of uncertainty (Li et al., 2012). For risks lacking a clear quantitative probability model, a fuzzy logic system can be used to model the cause-and-effect relationships, evaluate the level of risk exposure, and rank the main risks consistently, considering both available data and expert opinions (Shang and Hossen, 2013). Fuzzy AHP is an effective tool for handling imprecise, uncertain, or ambiguous data, as well as addressing the high nonlinearity and complexity of hazard systems (Yang et al., 2013). AHP is more tolerant of inconsistencies or contradictions in decision-making preferences. It can handle situations where decision criteria may overlap or conflict, allowing for a more comprehensive analysis of complex decision problems.

Fuzzy Comparison Matrix: This process begins by constructing a fuzzy pairwise comparison matrix for comparing the elements based on their relative importance by utilizing Triangular Fuzzy Numbers (TFNs). These numbers capture uncertainty and imprecision in judgments, with defined ranges of possible values such as l_{ij} (the lowest possible value of the comparison), m_{ij} (the most likely or central value- representing the expected value), and u_{ij} (the highest possible value).

$$\tilde{A} = \begin{bmatrix} 1 & \breve{a}_{12} & \cdots & \breve{a}_{1n} \\ \breve{a}_{21} & 1 & \cdots & \breve{a}_{2n} \\ \cdots & \cdots & 1 & \cdots \\ \breve{a}_{n1} & \breve{a}_{n2} & \cdots & 1 \end{bmatrix} \quad \text{Eq. 9}$$

The corresponding values for judgement matrix define the relative importance of the factors, are represented in Table 6.

Table 6. Fuzzy Comparison Matrix.

	Age	**Condition**	**ADT**	**Detour**	**Closure**
Age	(1, 1, 1)	(0.67, 1, 1.5)	(0.5, 0.67, 1)	(0.5, 0.67, 1)	(0.33, 0.4, 0.5)
Condition	(0.5, 1, 1.5)	(1, 1, 1)	(0.67, 1, 1.5)	(0.67, 1, 1.5)	(0.4, 0.5, 0.67)
ADT	(1, 1.5, 2)	(0.5, 1, 1.5)	(1, 1, 1)	(1, 1, 1)	(0.5, 0.67, 1)
Detour	(1, 1.5, 2)	(0.5, 1, 1.5)	(1, 1, 1)	(1, 1, 1)	(0.5, 0.67, 1)
Closure	(2, 2.5, 3)	(1.5, 2, 2.5)	(1, 1.5, 2)	(1, 1.5, 2)	(1 ,1 ,1)

Degree of Possibility Computation: Once we construct fuzzy matrix, the next step is to compare these fuzzy values. The main aim is to compute the degree of possibilities, which define how likely one Fuzzy Synthetic Extent Value (S_i) is greater than or equal to another. The formulation is as follows where i denote the row number, while j represents the column number.

$$S_i = \sum_{j=1}^{m} M_{gi}^{j} * \left[\sum_{i=1}^{n}\sum_{j=1}^{m} M_{gi}^{j}\right]^{-1} \quad \text{Eq. 10}$$

$$\sum_{j=1}^{m} M_{gi}^{j} = \left(\sum_{j=1}^{m} l_i, \sum_{j=1}^{m} m_i, \sum_{j=1}^{m} u_i\right) \quad \text{Eq. 11}$$

$$\left[\sum_{i=1}^{n}\sum_{j=1}^{m} M_{gi}^{j}\right]^{-1} = \left(\frac{1}{\sum_{j=1}^{n} l_i}, \frac{1}{\sum_{j=1}^{n} m_i}, \frac{1}{\sum_{j=1}^{n} u_i}\right) \quad \text{Eq. 12}$$

The determination of $S_1 = (l_1, m_1, u_1)$ and $S_2 = (l_2, m_2, u_2)$, where $S_1 \geq S_2$ can be expressed in Equation 12. This computation ensures that we quantify the overlap between the two fuzzy numbers, offering a mathematical approach to uncertainty management.

$$V(S_1 \geq S_2) = \left\{ \begin{array}{c} 1, \text{if } m_1 \geq m_2 \\ 0, \text{if } l_2 \geq u_1 \\ \dfrac{l_2 - u_1}{(m_1 - u_1) - (m_2 - l_2)}, \text{else} \end{array} \right\} \quad \text{Eq. 13}$$

Aggregating Degrees of Possibility Values: Each Fuzzy Synthetic Extent Value (S_i) is compared with all other fuzzy numbers in the matrix. The overall degree of possibility for a Synthetic Extent Value to be greater than all others is:

$$V(S \geq S_1, S_2, \ldots, S_k) = V(S \geq S_1)\ ;\ (S \geq S_2)\ ;\ \ldots ;\ (S \geq S_k) \quad \text{Eq. 14}$$

$$V = \min V(S \geq S_i) \text{ where } i = 1, 2, \ldots, k \quad \text{Eq. 15}$$

This step consolidates the pairwise comparisons into a singular value for each factor, indicating its overall significance in relation to all other factors. The application of the minimum value guarantees a conservative estimate, indicating that a factor's significance is assessed based on its least favorable comparison.

Computing Fuzzy Priority: The fuzzy priority ($d'(A_i)$) for each factor (A_i) is calculated to find the smallest degree of possibility $V(S_i \geq S_k)$ where S_k represents all other factors. This step ensures that each factor's priority corresponds to its dominance over all others. The minimum value approach focuses on a factor's weakest comparison, making the results more robust and realistic in the context of uncertainty. Our priority formula can be seen in Equation 16:

$$d'(A_i) = \min V(S_i \geq S_k), \text{where } k = 1, 2, \dots, n; k \neq i \quad \text{Eq. 16}$$

Constructing the Weight Vector: We created a fuzzy weight vector by combining the fuzzy priority indices for each factor. To find the weight of the factors (W'), Equation 17 is utilized. This vector represents the unnormalized importance of each factor. This is a preliminary step before obtaining our final weights.

$$W' = [d'(A_1), d'(A_2), \dots, d'(A_n)] \quad \text{Eq. 17}$$

Final Weight Factor Normalization: Finally, the fuzzy weights are normalized to convert them into crisp values that sum up to 1. This step ensures that the weights are directly comparable. The normalization formula is in Equation 18:

$$W(A_i) = \frac{d'(A_i)}{\sum W'} \quad \text{Eq. 18}$$

This step generates the final priority weights for each factor, which is utilized during the decision-making process. Normalization makes the results easier to interpret by ensuring the sum of all weights equals to 1.

2.6. Kernel Density Estimation for Closeness Distribution

Several visualization techniques are utilized to effectively convey the spatial distribution of flood-vulnerable bridges. County-level and point distribution maps clearly represent bridge locations, impact indices, and overall inundation patterns. Histograms and tables further complement these spatial analyses, providing a straightforward way to illustrate the processed data without the need for extensive methodological explanation. Kernel Density estimation, however, requires additional explanation due to its more complex statistical nature. Density analysis transforms point data into continuous spatial distributions, enabling the identification of high-impact clusters. The following section details the Kernel Density approach and its application to our analysis.

We utilized the Quartic Kernel Density Estimation, a method that provides a tool for estimating the shape of a probability density distribution based on a point set, to assess the flooding impact on bridges in Iowa (Silverman, 1986; Diggle, 1985, 1990). The Quartic Kernel was selected due to its capacity to effectively balance smoothness with local variation. The Quartic Kernel provides adequate detail preservation without creating discontinuities, in contrast to the highly localized Epanechnikov Kernel that produces blocky surfaces or the Gaussian Kernel that over-smooths distant points. The Quartic (Biweight) Kernel is mathematically defined in Equation 19:

$$K'(u) = w\frac{15}{16}(1 - u^2)^2 \text{ for } |u| \leq 1, K'(u) = 0 \text{ for } |u| > 1 \quad \text{Eq. 19}$$

In the equation above, K′(u) represents the weighted Kernel function, u is the normalized distance between the center of the Kernel and the point being evaluated as $u = d/h$, where d is the spatial separation between a bridge and the Kernel center, and h (the bandwidth or radius) controls the Kernel's smoothing effect. The Kernel is defined to have a value of zero for distances $|u|>1$, meaning that the influence of a point is limited to a defined bandwidth h. The weight w corresponds to impact index, ensuring that high-impact bridges exert greater influence on density estimates. Using weights derived from the Analytical Hierarchy Process, Fuzzy AHP impact indices, and census block population data ensures that both population distribution and bridges with higher impact indices contribute more significantly to the estimated density.

To provide a basis for comparison, we also utilized bridge inundation data (without weights) to highlight the relationships and differences between the weighted and unweighted approaches. The weighting approach emphasizes areas where flooding would have the most severe consequences, allowing the density map to highlight regions with high concentrations of heightened vulnerability. This facilitates the identification of critical hotspots that reflect both structural distribution and the significance of individual bridges. To illustrate the functionality of Kernel Density estimation, we provide a visual representation of bridge locations alongside their relative density estimates, as shown in Figure 2.

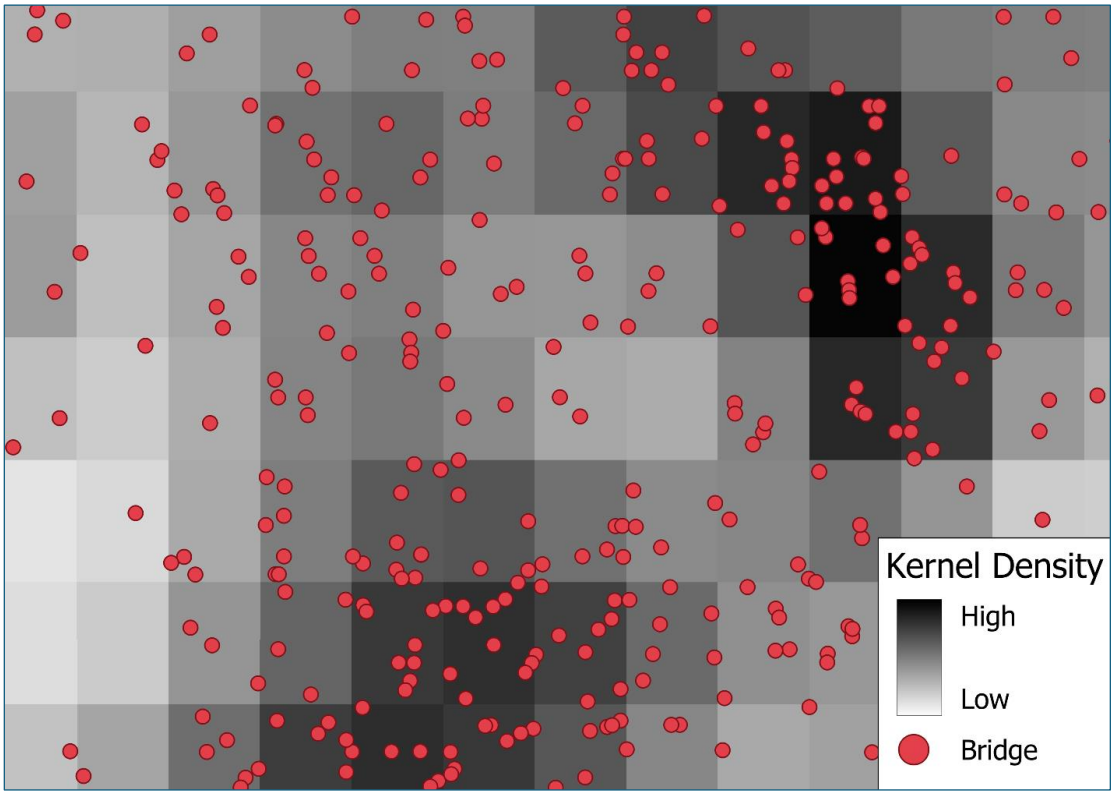

Figure 2. Kernel closeness distribution illustration.

As can be seen, the grayscale background displays the Kernel Density, with darker regions denoting higher density values, and red points indicate the locations of bridges. Areas with a high

density of data points are highlighted by the darker areas, which are the result of the spatial autocorrelation effect of nearby bridges. Furthermore, the smoothing effect of the bandwidth is reflected in the gradual changes between density levels, guaranteeing that nearby bridges also aid in density estimation. To make the concept more understandable, the illustration is shown on a large scale with a high bandwidth; however, in real-world analyses, the bandwidth selection is crucial to successfully balancing smoothness and local detail.

3. Results and Discussion

This section provides a detailed description of the vulnerability assessment of bridge inundation in Iowa. It represents county-level flood exposure, impact index distributions at both bridge and county scales, and spatial impact patterns through Kernel Density analysis. The findings illustrate flood-prone areas, highlight variations across different evaluation methods, and support infrastructure resilience planning.

3.1. Bridge Inundation and County Condition

This section presents a county-scale analysis of bridge inundation percentages during a 500-year flooding scenario in Iowa. Counties were chosen for analysis as bridges are governed and maintained at the county and state levels, enabling a more precise evaluation of flooding impacts within their jurisdiction. Figure 3 illustrates these percentages across Iowa, highlighting counties with the highest bridge closure rates.

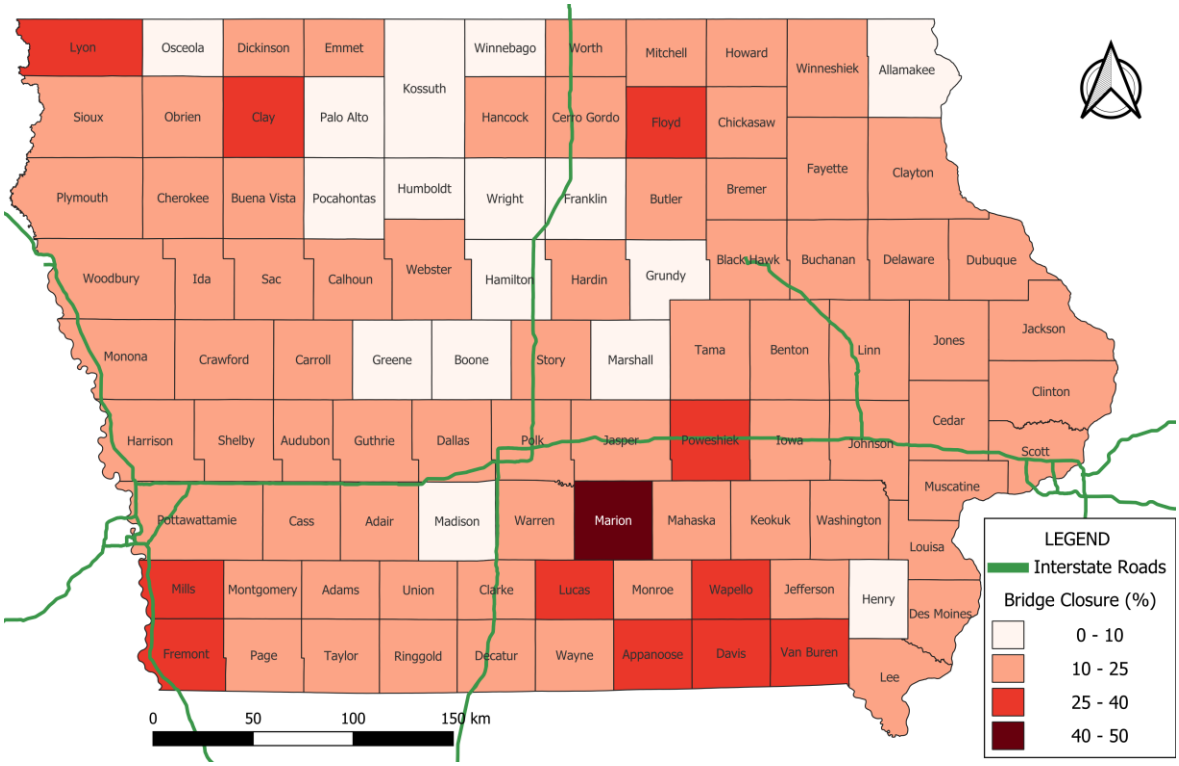

Figure 3. County bridge inundation percentage for at least single flood scenario.

A spatial analysis of bridge closures, as shown in Figure 3, reinforces these findings in the context of a 500-year flooding scenario. An important distinction between rural and urban areas is revealed by the examination of bridge closures. Forty of Iowa's 99 counties are classified as rural, a classification that is crucial for the development of flood mitigation strategies, according to the USDA (U.S. Department of Agriculture). Rural counties are vulnerable to extreme drought and flooding events, such as a 500-year flood scenario, as evidenced by their high absolute closures and high closure percentages (Islam et al., 2024). These counties, which have fewer bridges, experience disproportionately high flooding impacts, with additional constraints due to limited resources for flood management. The map emphasizes that rural counties in central and southern Iowa, including Marion, Lucas, and Appanoose, are particularly susceptible to flooding due to their high closure percentages relative to their bridge networks.

Urban counties such as Johnson (72 bridges closed, 19.89%) and Woodbury (73 bridges closed, 16.11%) exhibit lower closure percentages, despite having a high number of closed bridges. This is indicative of the significantly larger and more resilient infrastructure systems of urban areas, which are facilitated by improved flood management practices, more frequent maintenance, and larger budgets for infrastructure enhancements. These factors contribute to the reduction of flooding's impact, which leads to reduced relative closure rates in counties with extensive bridge networks. In addition, border counties, including Lyon, Mills, Fremont, Appanoose, Davis, and Van Buren, are particularly important for interstate connectivity and regional transportation. Mills, Fremont, and Poweshiek counties are distinguished by their elevated bridge closure rates, which, when coupled with the presence of critical interstate highways, underscore their critical significance to both regional and national transportation networks.

To gain a more comprehensive understanding of the critical flood impacts, it is possible to examine the counties with the highest number of bridge closures. Table 7 emphasizes the counties with the highest total closures and closure percentages, accentuating their vulnerability during extreme flooding events, while the map illustrates flood severity.

Table 7. Top Ten Counties for Inundated Bridge Number and Percentage During 500-year Flood.

County	**#Bridges**	**#Closed**
Marion	216	102
Pottawattamie	565	94
Jasper	377	91
Sioux	448	89
Clinton	372	80
Lucas	196	77
Poweshiek	263	77
Woodbury	453	73
Johnson	362	72
Appanoose	188	70

County	**#Bridges**	**%Closed**
Marion	216	47.22
Lucas	196	39.29
Appanoose	188	37.23
Davis	171	36.26
Fremont	171	35.67
Clay	155	34.84
Van Buren	157	31.21
Mills	180	30.56
Poweshiek	263	29.28
Lyon	272	25.37

Among the counties with the highest total number of closed bridges, Pottawattamie, Jasper, Sioux, and Clinton top the list. These counties have large number of bridges, which leads to a high number of absolute closures. Nevertheless, the vulnerability of rural counties becomes evident when comparing the percentage of inundated closures to the total number of bridges, as the analysis reflects bridges that are inundated in at least one flood scenario. Marion, Lucas, Poweshiek, and Appanoose all appear in the top 10 for the total number of closed bridges and the percentage of closures. Particularly, Marion County stands out with 102 closed bridges, representing almost half of its total bridges, making it the county with the highest percentage of closure.

This suggests that Marion's bridge inventory is relatively smaller, which means that a greater volume of its infrastructure is vulnerable to flooding during extreme events like the 500-year flood scenario. Other rural counties, including Lucas and Appanoose, also experience substantial disruption because of higher closure percentages. Davis, Fremont, and Clay are among the rural counties that have fewer bridges but high closure percentages, which further exacerbates their vulnerability. Notably, Poweshiek and Lyon show moderate numbers of closed bridges but still have considerable closure percentages, particularly Poweshiek, which ranks high on both metrics. The findings emphasize the need for targeted flood mitigation efforts, particularly in rural and border areas, to safeguard infrastructure and reduce future disruptions caused by severe flooding events.

3.2. AHP and Fuzzy AHP Weight Distribution

This section presents the weights assigned to the bridge parameters using two different multi-criteria decision-making methodologies: AHP (Analytic Hierarchy Process) and Fuzzy AHP. The comparison highlights the differences in how each method prioritizes factors. Fuzzy AHP allows us to adjust the weights of criteria and alternatives based on their degree of certainty, with the weights being distributed more smoothly than traditional AHP, as shown in Table 8. Unlike traditional AHP, where weights are typically assigned using pairwise comparisons based on crisp numerical scales, Fuzzy AHP allows for gradual adjustments of weights. This gradual adjustment process ensures smoother transitions between different weighting configurations and helps capture subtle variations in decision criteria importance. Moreover, sensitivity analysis helps identify optimal weighting configurations and enhances decision robustness. The relative importance of criteria can be expressed more context-sensitively as a result of this flexibility, which allows for the incremental fine-tuning of the weights of criteria and alternatives in accordance with their changing circumstances or evolved preferences.

According to Table 8, the changes in weight between AHP and Fuzzy AHP, particularly for Closure and Condition, demonstrate how the methodologies affect the weight distribution. Closure shows a significant decrease in weight from AHP to Fuzzy AHP. This suggests that incorporating uncertainty slightly reduces the prominence of closure. ADT and Detour have nearly identical weights in both methods, indicating that these parameters remain stable regardless of the inclusion of uncertainty. On the other hand, Condition and Age both show an increase in weight in Fuzzy AHP compared to AHP. This shift indicates that Fuzzy AHP tends to assign slightly more

importance to these parameters than AHP, due to how Fuzzy AHP accounts for uncertainty in decision-making. Despite this increase, their weights remain lower than the other parameters like closure and traffic because both methods use the same hierarchy base.

Table 8. AHP and Fuzzy AHP Weight Distribution.

Parameter/Weight	AHP	Fuzzy AHP
Closure	0.456	0.379
ADT	0.185	0.186
Detour	0.185	0.186
Condition	0.108	0.161
Age	0.067	0.088

3.3. Impact Index Distribution on Bridge Scale

This analysis focuses on evaluating the vulnerability of inundated bridges during a 500-year flood event in Iowa by assessing the impact of bridge closures and related disruptions. To evaluate this, impact indices for the bridges are calculated using AHP and Fuzzy AHP. The maps presented below visualize the geographic distribution of these bridge impact indices across the state, offering a clear representation of how each methodology assigns indices to bridges in different regions.

Although both approaches have similar foundations, the results of the comparative study of the maps in Figure 4 created using AHP and Fuzzy AHP demonstrate significant distinctions in the way bridge susceptibility to flooding is evaluated. The parameters, classification schemes, and hierarchy of both maps are similar; however, since Fuzzy AHP incorporates uncertainty through membership functions, their computation mechanisms are different. This results in different patterns of vulnerability and emphasizes how crucial it is to use both methods for a more complete impact assessment.

A key difference between these two methods is how they assign impact indices, which can be seen in the color variations on the maps. Fuzzy AHP generally produces lower impact indices than AHP. That means the same bridges may fall into different index ranges. This happens because Fuzzy AHP accounts for uncertainty and reduces the influence of extreme values, which are more noticeable in AHP results. In high-risk areas identified by AHP, Fuzzy AHP provides a more detailed breakdown, highlighting local variations in vulnerability. This detail helps identify subtle differences within areas that might otherwise seem homogeneous. AHP tends to emphasize bridges near urban centers, especially in central Iowa, prioritizing their proximity to critical infrastructure. In contrast, Fuzzy AHP shifts focus to rural areas, particularly in central and southwestern Iowa, where it uncovers hidden vulnerabilities. This shows how Fuzzy AHP can reveal risks that may not be as obvious in AHP.

While the maps provide a valuable visual representation of the spatial distribution of bridge impact indices across Iowa, they do not capture the full index distribution due to binning within specific intervals. To complement this analysis, the next section presents histograms that illustrate

the accumulation of indices, offering a more detailed understanding of how the methodologies distribute bridge indices across different intervals and impact levels.

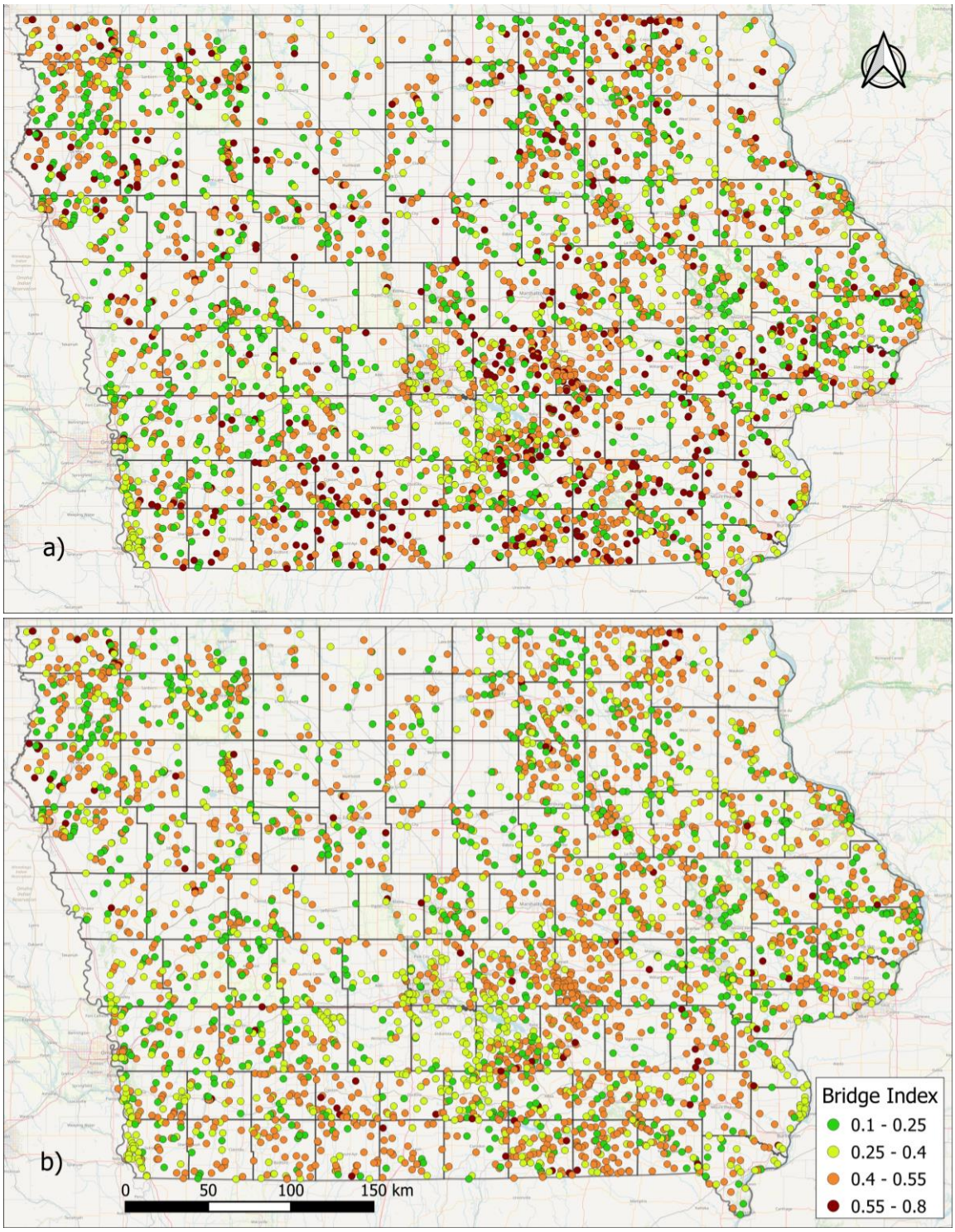

Figure 4. Bridge index distribution for: a) AHP method; b) Fuzzy AHP method.

According to the histograms, the distribution of bridge impact indices differs between the two methodologies, with Fuzzy AHP resulting in a smoother, more well-distributed pattern compared to the more clustered distribution from AHP. In the lower range, AHP assigns a significant portion of bridges to this interval, with indices near the lower end of the scale being disproportionately represented. For instance, 21 bridges fall within the 0.160–0.165 interval, while there is no bridge is assigned to the 0.140–0.145 range. In contrast, Fuzzy AHP spreads the indices more evenly across the lower range. This wider distribution indicates that Fuzzy AHP is less likely to overemphasize lower indices, likely due to the smoother transitions reduces sharp distinctions between parameters.

As shown in Figure 5, the distribution of AHP scores reveals a more concentrated grouping in the middle range, particularly between 0.170 and 0.250. Additionally, there are noticeable gaps in the distribution in the intervals 0.300–0.310 and 0.435–0.465. This lack of smooth transition can lead to a less precise representation of bridge conditions. Fuzzy AHP, by contrast, distributes indices more evenly across the middle range without such dips, demonstrating its ability to handle variability and uncertainty in the evaluation process.

AHP exhibits a skew towards higher indices in the upper range, with a significant portion of bridges falling between 0.395 and 0.465. This clustering suggests that AHP's rigid ranking system leads to a narrower distribution. Fuzzy AHP presents a more balanced distribution, gradually extending into the upper index ranges and avoiding sharp concentrations in specific intervals. The higher end of the spectrum shows more balanced distribution, with 57 bridges assigned here, compared to AHP's tendency to concentrate indices in narrower ranges.

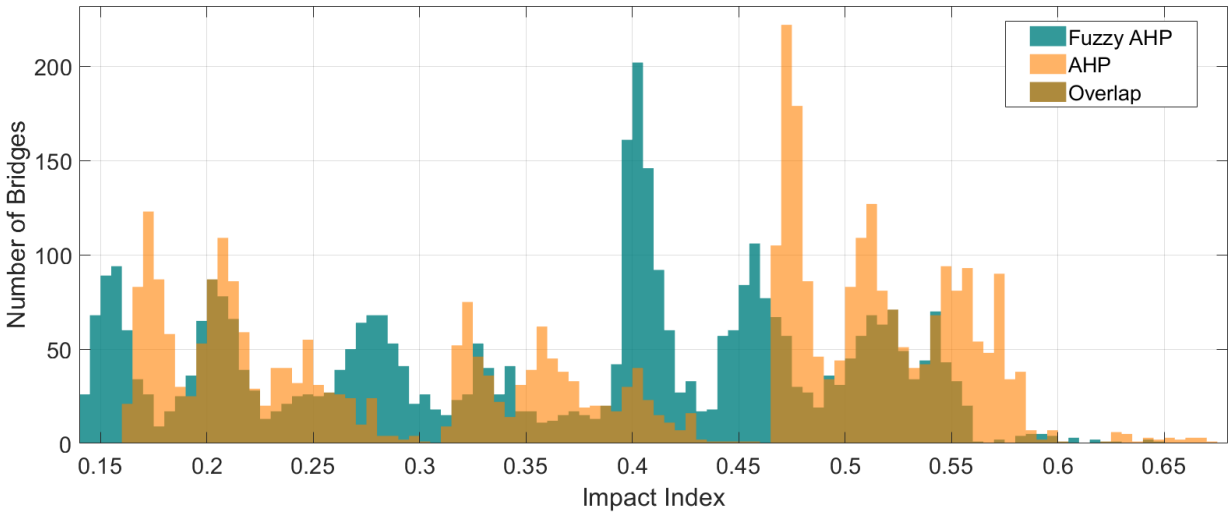

Figure 5. AHP and Fuzzy AHP Impact Index Distribution for Bridges.

The comparison between AHP and Fuzzy AHP highlights key differences in how they assess bridge vulnerability. AHP excels quickly identifying broad, high-risk areas. On the other hand, with its incorporation of fuzzy logic, Fuzzy AHP adds depth by accounting for uncertainties, offering a more refined impact computation. Together, these methods provide complementary

perspectives, enhancing decision-making and offering a more reliable, layered framework for flood risk evaluation.

3.4. Impact Index Distribution at County Scale

To assess the overall impact of bridge inundation, we present both general and inundation indices, enabling us to identify counties where inundation indices are high while overall indices remain low. This highlights counties with a low percentage of bridge closures but where the remaining bridges hold significant impact indices, indicating their potential to cause critical disruptions. Since bridges are dependent on county authorities, analyzing impacts at the county level is essential for understanding the broader effects of bridge inundation and guiding effective decision-making. Figure 6 provides a visual representation of the county-level impact index distribution, highlighting the geographic variations in vulnerability. These maps illustrate how the AHP and Fuzzy AHP methodologies assess the spatial distribution of bridge impacts differently, revealing key areas with significant variations in vulnerability.

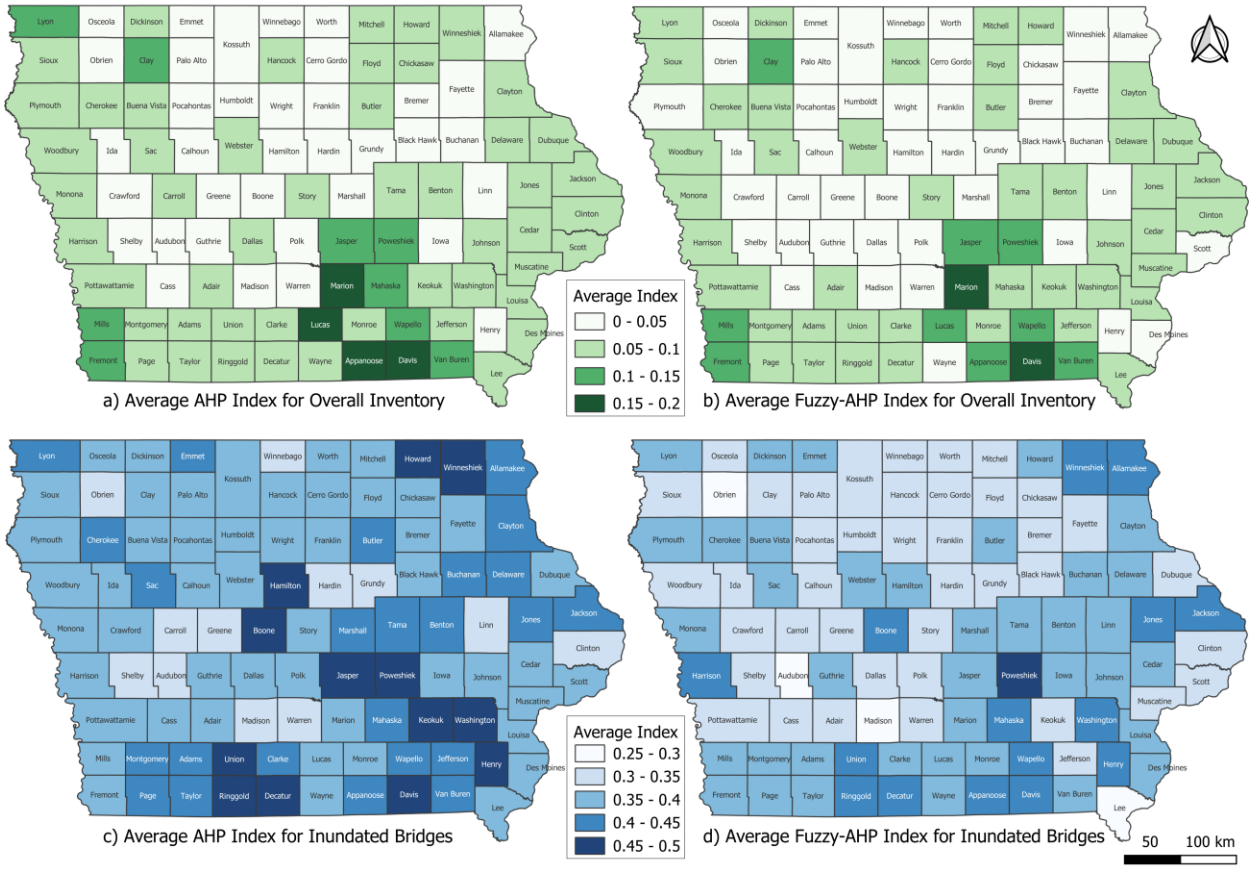

Figure 6. Impact index distribution for Iowa counties.

According to Figure 6, when we compare the overall inventory indices to the inundated inventory indices across both the AHP and Fuzzy methods, it is highlighted the counties with dramatic shifts in ranking due to the vulnerability of their infrastructure during extreme flooding

events. These changes highlight how crucial both models are for capturing the risks associated with flood impact.

Starting with the AHP model, Poweshiek County in central Iowa stands out with a significant shift in its ranking. While the county shows moderate vulnerability in its overall inventory, it rises to the highest average impact index in the inundated inventory. This illustrates how localized flooding can severely impact counties with fewer bridges, significantly raising their inundation inventory indices. On the Fuzzy AHP side, the shift is even more pronounced. Poweshiek again rises sharply in its inundated inventory despite its relatively low rank in the all-inventory index. In contrast, Marion County, located in south-central Iowa, ranks highly in terms of its all-network impact, but shows a more moderate shift in the inundated inventory, indicating that the county does not experience as severe an increase in its inundation-specific vulnerability. This suggests that Marion's inundated inventory includes a significant number of bridges with low impact indices, which allows it to maintain a moderate vulnerability across both models.

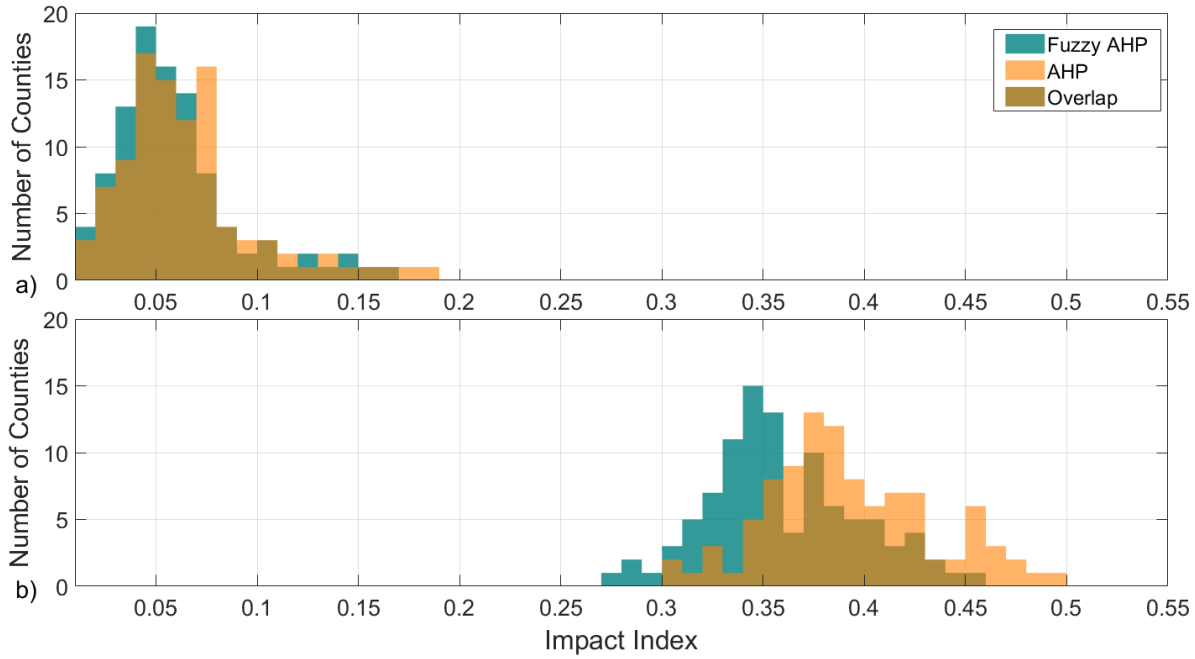

Figure 7. County-wise Average Impact Index Distribution for: a) All Bridge Inventory; b) Only Inundated Bridges.

Another key county reflecting a shift in rankings is Davis County in the southeastern region. Davis has a relatively high overall vulnerability with an AHP impact index, and its inundated inventory sees a substantial increase. Fuzzy AHP index evaluation amplifies the same trend, showing the impact of flooding on the county's bridges. Although Davis doesn't have the most extensive bridge network, the inundated impacts place it among the highly vulnerable counties. On the other hand, the border counties such as Howard, Winneshiek, Ringgold, and Decatur show significant jumps in inundated inventory indices, highlighting their vulnerability despite relatively low overall inventory impact indices. These changes emphasize how localized flooding

significantly impacts these counties, making them more vulnerable despite their smaller overall bridge networks. Their border locations amplify the risk, requiring targeted flood mitigation to protect regional connectivity.

The maps offer valuable insights into the geographic distribution of bridge flood susceptibility, as in the previous section. However, they do not fully capture the distribution of indices across intervals within counties. To complement this, the histograms in Figure 7 present the accumulation of impact indices, offering a more detailed understanding of how the counties' indices are distributed and highlighting shifts in vulnerability between the overall and inundated bridge inventories.

The analysis of the county-level average impact indices for both the overall and inundated bridge inventories reveals distinct patterns in the distribution of vulnerability. In the overall inventory, which includes both inundated and non-inundated bridges, most counties have indices between 0.04 and 0.06 for both AHP and Fuzzy AHP. The prevalence of these lower average indices is due to the non-inundated bridges, which do not have impact indices. The highest indices in this group are between 0.10and 0.11, but only a few counties fall in this range. When considering only the inundated bridges, in both the AHP and Fuzzy AHP, a significant number of counties are found in the 0.34-0.38 range. Specifically, 13 counties are in the 0.37-0.38 interval for AHP, and 15 counties are in the 0.34-0.35 interval for Fuzzy AHP average impact indices. Additionally, six counties fall into the 0.45–0.46 range, creating a sudden peak that is important to evaluate.

The combination of maps and histograms provides a comprehensive view of the flood impact on bridges across Iowa. The maps offer insights into the geographic distribution of vulnerability, highlighting areas that are more susceptible to flooding, while the histograms give a detailed breakdown of how these vulnerabilities vary within different counties. Together, these tools highlight the need for a detailed approach to flood risk management. They emphasize the importance of both spatial and quantitative assessments. Combining these methods helps to better understand and address local risks.

3.5. Kernel Density Analysis

We generated four Kernel Density maps using data from over 3,800 inundated bridges affected by at least one flood scenario in Iowa: one with just the inundation data and the others with AHP impact index, Fuzzy AHP impact index, and population weighted in. We wanted to capture smooth variations in the density of inundated bridges using our point-based data, focusing on both the weighted impact factors and the proximity to flood-prone areas.

In Figure 8, the Kernel Density maps provide a comparative visualization of flood-vulnerable bridges in Iowa. The unweighted inundation map (Figure 8.a) shows the baseline distribution of flood-exposed bridges. The AHP (Figure 8.b) and Fuzzy AHP (Figure 8.c) maps enhance this analysis by incorporating structural importance and traffic disruption. The population-weighted map (Figure 8.d) adds further perspective by emphasizing human exposure to bridge closures. When combined, these maps provide a multifaceted understanding of bridge flood vulnerability,

highlighting both typical high-impact areas and notable differences between multiple assessment techniques.

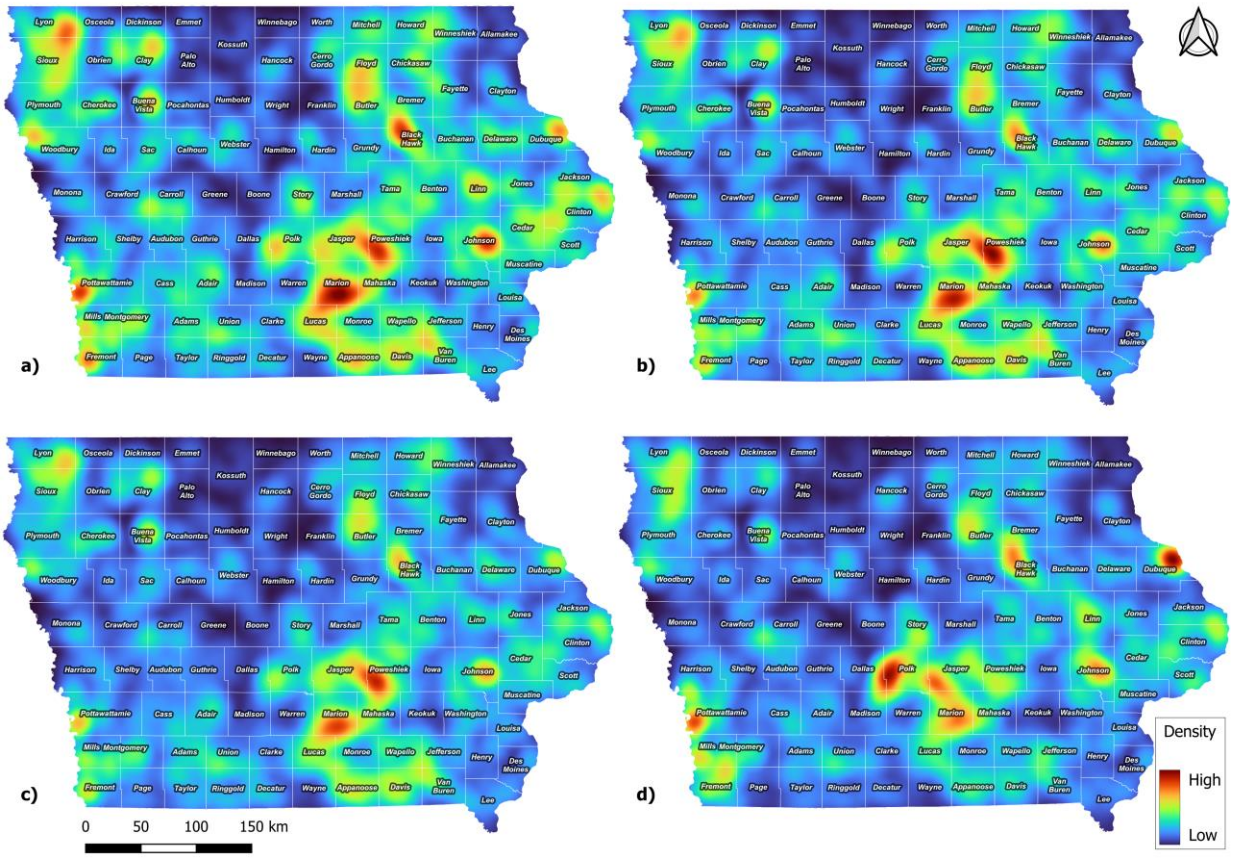

Figure 8. Kernel Density Distribution for Bridge Inundation: a) Unweighted; b) AHP weighted; c) Fuzzy AHP weighted; d) CENSUS Block Group Population Weighted.

The unweighted inundation density map reveals key clusters of flood-affected bridges, primarily concentrated in Marion County, which stands out as the most intense hotspot. Another significant accumulation appears along the border of Pottawattamie and Fremont Counties, indicating severe flood impacts in these southwestern areas. Moreover, notable hotspots emerge in Iowa City (Johnson County), Black Hawk County, and the lower left section of Poweshiek County. These patterns reflect regions where inundation is most frequent.

When incorporating AHP and Fuzzy AHP weightings, there are notable shifts in high-density zones. Poweshiek County surpasses Marion County as the most flood-vulnerable area in the AHP-weighted map, indicating that bridges in this region have higher impact indices due to structural concerns or traffic disruptions. Fuzzy AHP preserves the general pattern of AHP but introduces refinements, maintaining Poweshiek and Marion as dominant hotspots while additional vulnerable zones appear such as the border counties Appanoose, Davis, and Pottawattamie. The increased prominence of these rural counties suggests that fuzzy logic captures localized vulnerabilities.

The population-weighted Kernel Density map provides an additional perspective on flood impact by incorporating census block population data rather than larger census tracts or county-level data. This finer granularity aids us to capture a more localized representation of population exposure, allowing for a more precise understanding of how bridge inundations affect communities. However, population was not included in the impact index calculation because Annual Daily Traffic (ADT) offers a more direct measure of disruption, reflecting actual bridge usage rather than nearby residential density. Instead, population data is presented as a complementary layer to highlight areas where bridge closures may have broader societal consequences.

This distinction explains why the highest-density areas in the population-weighted map shift toward Polk County (Des Moines) and Dubuque County, where higher population densities amplify the perceived flood impact. Meanwhile, previously critical areas like Poweshiek County have become less prominent due to lower residential density, despite their structural vulnerability. Pottawattamie County remains a critical hotspot, reinforcing its significance both in terms of infrastructure and population exposure. By incorporating population separately, this analysis provides a more balanced perspective, ensuring that both structural vulnerability and human accessibility concerns are accounted for in flood risk assessments.

4. Conclusion

This study highlights the importance of integrating multiple impact evaluation methodologies to capture both structural vulnerability and transportation disruptions. By analyzing bridge inundation, impact index distributions, and their spatial variations, this study provides a critical foundation for improving flood mitigation strategies for the Iowa transportation network. A comprehensive, data-driven approach is required to reduce disruptions and improve resilience against future flooding events, allowing decision-makers to prioritize and strengthen vulnerable bridges.

The analysis of bridge closures reveals a significant distinction between rural and urban areas. Rural counties exhibit both high absolute closures and high closure percentages, highlighting their vulnerability during flooding events. These counties, with fewer bridges, face disproportionately high impacts from flooding, further exacerbated by limited resources for flood management. Border counties are particularly critical because of their strategic role in regional transportation and interstate commerce. While urban areas generally benefit from more resilient infrastructure, the study highlights the need for targeted flood mitigation efforts in rural and border regions to safeguard infrastructure and reduce future disruptions

By comparing AHP and Fuzzy AHP methodologies, the study justifies their integration for a more robust flood vulnerability assessment. While similarities in classification and parameter hierarchies exist as expected the impact index evaluation differences and resulting spatial variations are key to obtaining a more comprehensive understanding of flood vulnerability. The value of integrating both methodologies for a robust and multidimensional evaluation is further emphasized by these insights. The AHP and Fuzzy AHP models offer valuable insights into the

vulnerabilities faced by counties, revealing a complex relationship between inundated bridge vulnerability and overall infrastructure impact.

Counties such as Poweshiek and Davis show how flooding can push counties with smaller bridge networks into a high-risk category, despite their relatively lower overall vulnerability. In contrast, counties like Marion exhibit a more moderate shift, suggesting that while they have a larger bridge network, their infrastructure is somewhat more resilient to flooding. The impact indices, particularly for border counties like Howard and Winneshiek in the north and Ringgold and Decatur in the southeast, demonstrate how flooding can disproportionately impact regions crucial for interstate transportation and regional connectivity.

Moreover, the Kernel Density analysis highlights key flood-prone areas in Iowa, with Marion, Poweshiek, Pottawattamie, and Fremont Counties emerging as critical hotspots across different weighting methods. The unweighted map establishes fundamental inundation patterns, while AHP and Fuzzy AHP refine the assessment by prioritizing structurally significant and high-traffic bridges. The population-weighted map directs attention to urban areas such as Polk and Dubuque Counties, emphasizing human exposure but underrepresenting critical rural infrastructure. These findings underscore the value of using multiple methodologies to assess flood risk comprehensively, ensuring that both structural vulnerability and community accessibility are considered in infrastructure resilience planning.

Overall, this study emphasizes the necessity of a balanced flood risk management strategy that addresses both immediate structural concerns and broader societal impacts. Our findings indicate the need for a detailed approach to flood risk management that considers not only overall infrastructure exposure but also the localized impacts of flooding in counties with smaller or more critical bridge networks. While it offers a comprehensive assessment of bridge vulnerability, further research is needed to refine these insights.

Future studies could incorporate dynamic flood modeling (Krajewski et al., 2021) to account for real-time hydrological changes and climate variability, improving predictive accuracy. Temporal analyses of past flood events and infrastructure performance could help validate impact indices and reveal long-term resilience trends. Additionally, assessing the economic consequences of bridge closures, such as supply chain disruptions and emergency response delays, would offer a more holistic understanding of flood impacts. Finally, exploring alternative mitigation strategies, such as adaptive bridge designs and flood controls could further strengthen infrastructure resilience in high-risk rural and border counties.

5. References

Alabbad, Y., Yildirim, E., & Demir, I. (2023). A web-based analytical urban flood damage and loss estimation framework. *Environmental Modelling & Software*, *163*, 105670.

Alabbad, Y., Mount, J., Campbell, A. M., & Demir, I. (2024). A web-based decision support framework for optimizing road network accessibility and emergency facility allocation during flooding. *Urban Informatics*, *3*(1), 10.

Alabbad, Y., & Demir, I. (2024). Geo-spatial analysis of built-environment exposure to flooding: Iowa case study. *Discover Water*, *4*(1), 28.

Botzen, W. W., Deschenes, O., and Sanders, M. (2019). The economic impacts of natural disasters: A review of models and empirical studies. Review of Environmental Economics and Policy, 13 (2), 167–188. https://doi:10.1093/reep/rez004.

Chang, D. Y. (1996). Applications of the extent analysis method on fuzzy AHP. European Journal of Operational Research, 95(3), 649– 655. https://doi.org/10.1016/0377-2217(95)00300-2.

Cikmaz, A. B., Alabbad, Y., Yildirim, E., & Demir, I. (2024). A Comprehensive Flood Risk Assessment for Railroad Network: Case Study for Iowa. EarthArxiv, 6427. https://doi.org/10.21203/rs.3.rs-4171938/v1

Cikmaz, B. A., Yildirim, E., & Demir, I. (2023). Flood susceptibility mapping using fuzzy analytical hierarchy process for cedar rapids, Iowa. International journal of river basin management, 1-24. https://doi.org/10.1080/15715124.2023.2216936.

Crawford, S. E., Brinkmann, M., Ouellet, J. D., Lehmkuhl, F., Reicherter, K., Schwarzbauer, J., ... & Hollert, H. (2022). Remobilization of pollutants during extreme flood events poses severe risks to human and environmental health. Journal of Hazardous Materials, 421, 126691.

D. Rinc´on, U.T. Khan, C. Armenakis, Flood risk mapping using GIS and multi-criteria analysis: a greater Toronto area case study, Geosciences 8 (8) (2018) 275.

Das, P. (2010). Selection of business strategies for quality improvement using fuzzy analytical hierarchy process. International Journal for Quality Research, 4(4), 283–292.

Diggle, P. J. (1985), A kernel method for smoothing point process data: Applied Statistics, v. 34, no. 2, p. 138-147.

Diggle, P. J. (1990), A point process modelling approach to raised incidence of a rare phenomenon in the vicinity of a pre-specified point: Jour. Roy. Statis. Sot., Ser. A, v. 53, no. 3, p. 349-362.

Doorga, J. R. S., Magerl, L., Bunwaree, P., Zhao, J., Watkins, S., Staub, C. G., Rughooputh, S. D. D. V., Cunden, T. S. M., Lollchund, R., & Boojhawon, R. (2022). GIS-based multi-criteria modelling of flood risk susceptibility in Port Louis, Mauritius: Towards resilient flood management. International Journal of Disaster Risk Reduction, 67, 102683. https://doi.org/10.1016/j.ijdrr.2021.102683

Duran, E., Alabbad, Y., Mount, J., Yildirim, E., & Demir, I. (2025). Comprehensive analysis of riverine flood impact on bridge and transportation network: Iowa case study. International Journal of River Basin Management, 1-14. https://doi.org/10.1080/15715124.2025.2457546.

Duran, E., Demir, I. (2024). Comprehensive assessment of flood impact, zonal statistics, and site suitability for wind turbines in Iowa. EarthArxiv, 7981. https://doi.org/10.31223/X5R12B.

Engel, A., Last, M., 2007. Modeling software testing costs and risks using fuzzy logic paradigm. J. Syst. Softw. 80 (6), 817–835.

G. Papaioannou, L. Vasiliades, A. Loukas, Multi-criteria analysis framework for potential flood prone areas mapping, Water Resour. Manag. 29 (2) (2015) 399–418.

Garlock, M., Paya-Zaforteza, I., Kodur, V., Gu, L., 2012. Fire hazard in bridges: Review, assessment and repair strategies. Eng. Struct. 35, 89–98. https://doi.org/10.1016/j.engstruct.2011.11.002.

GeoTREE. (2007). Iowa Lidar Mapping Project. Retrieved from http://www.geotree.uni.edu/lidar.

Gilles, D., Young, N., Schroeder, H., Piotrowski, J., & Chang, Y. J. (2012). Inundation mapping initiatives of the Iowa Flood Center: Statewide coverage and detailed urban flooding analysis. Water, 4(1), 85-106. https://doi.org/10.3390/w4010085

Highfield, W. E., & Brody, S. D. (2017). Determining the effects of the FEMA Community Rating System program on flood losses in the United States. International journal of disaster risk reduction, 21, 396-404. https://doi.org/10.1016/j.ijdrr.2017.01.013.

Huntsinger, L. F. (2022). Transportation systems planning. Highway Engineering (Second Edition), 17-81. https://doi.org/10.1016/B978-0-12-822185-3.00008-X

Iowa DOT (2015). Bridge Inspection Manual. Retrieved online at: https://iowadot.gov/siims/Bridge-Inspection-Manual

Iowa.gov. (2019). Office Of the Governor of Iowa. Retrieved from https://governor.iowa.gov/2019/03/governor-reynolds-launches-211-flood-hotline-and-one-stop-2019-iowa-floods-website-to-assist.

Islam, S. S., Yeşilköy, S., Baydaroğlu, Ö., Yıldırım, E., & Demir, I. (2024). State-level multidimensional agricultural drought susceptibility and risk assessment for agriculturally prominent areas. *International Journal of River Basin Management*, 1-18.

Khosravi, K., Shahabi, H., Pham, B. T., Adamowski, J., Shirzadi, A., Pradhan, B., ... & Prakash, I. (2019). A comparative assessment of flood susceptibility modeling using multi-criteria decision-making analysis and machine learning methods. *Journal of Hydrology*, *573*, 311-323.

Krajewski, W. F., Ghimire, G. R., Demir, I., & Mantilla, R. (2021). Real-time streamflow forecasting: AI vs. Hydrologic insights. *Journal of Hydrology X*, *13*, 100110.

Kuckartz, U., Rädiker, S., Ebert, T., Schehl, J., Kuckartz, U., Rädiker, S., ... & Schehl, J. (2013). Korrelation: Zusammenhänge identifizieren. Statistik: Eine verständliche Einführung, 207-237

Lebbe, Mohamed Farook Kalendher and Lokuge, Weena and Setunge, Sujeeva, and Zhang, Kevin (2014) Failure mechanisms of bridge infrastructure in an extreme flood event. In: Proceedings of the 1st International Conference on Infrastructure Failures and Consequences, 16-20 July 2014, Melbourne, pp124-132. ISBN: 978-0-9925570-1-0

Li, K., Wu, S., Dai, E., & Xu, Z. (2012). Flood loss analysis and quantitative risk assessment in China. Natural Hazards, 63(2), 737–760. https://doi.org/10.1007/s11069-012-0180-y

Li, Z., Xiang, Z., Demiray, B. Z., Sit, M., & Demir, I. (2023a). MA-SARNet: A one-shot nowcasting framework for SAR image prediction with physical driving forces. ISPRS journal of photogrammetry and remote sensing, 205, 176-190.

Li, Z., Duque, F. Q., Grout, T., Bates, B., & Demir, I. (2023b). Comparative analysis of performance and mechanisms of flood inundation map generation using Height Above Nearest Drainage. *Environmental Modelling & Software*, *159*, 105565.

Liu, H.-T., Tsai, Y.-L., 2012. A fuzzy risk assessment approach for occupational hazards in the construction industry. Safety Sci. 50 (4), 1067–1078.

Malczewski, J. (1999). GIS and multicriteria decision analysis. John Wiley & Sons, Inc.

Mitchell, B. Integrated Water Resource Management, Institutional Arrangements, and Land-Use Planning. Environ. Plan. A Econ. Sp. 2005, 37, 1335–1352.

Ozyuksel Ciftcioglu, A., & Naser, M. Z. (2024). Identifying and estimating causal effects of bridge failures from observational data. Journal of Infrastructure Intelligence and Resilience, 3(1), 100068. https://doi.org/10.1016/j.iintel.2023.100068

P. Adhikari, Y. Hong, K.R. Douglas, D.B. Kirschbaum, J. Gourley, R. Adler, G.R. Brakenridge, A digitized global flood inventory (1998–2008): compilation and preliminary results, Nat. Hazards 55 (2) (2010) 405–422.

Pourghasemi HR, Pradhan B, Gokceoglu C (2012) Application of fuzzy logic and analytical hierarchy process (AHP) to landslide susceptibility mapping at Haraz watershed, Iran. Nat Hazards. https://doi:10.1007/s11069-012-0217-2.

Pregnolato, M., Sarhosis, V., & Kilsby, C. (2018). Towards integrating modelling of flood induced bridge failures. In EPiC Series in Engineering 13th International Conference on Hydroinformatics (Vol. 3, pp. 1698-1702). Sadiq, R., & Tesfamariam, S. (2009). Environmental decision-making under uncertainty using intuitionistic fuzzy analytic hierarchy process (IF-AHP). Stochastic Environmental Research and Risk Assessment, 23(1), 75-91.

Putra, D., Sobandi, M., Andryana, S., & Gunaryati, A. (2018). Fuzzy analytical hierarchy process method to determine the quality of gemstones. Advances in Fuzzy Systems, 2018. https://doi.org/10.1155/ 2018/9094380.

Rentschler, J., Salhab, M., & Jafino, B. A. (2022). Flood exposure and poverty in 188 countries. Nature communications, 13(1), 3527. https://doi.org/10.1038/s41467-022-30727-4.

Saaty, R. W. (1987). The analytic hierarchy process—What it is and how it is used. Mathematical Modelling, 9(3–5), 161–176. https://doi.org/10.1016/0270-0255(87)90473-8

Saaty, T. L. (1980). The analytic hierarchy process (AHP). The Journal of the Operational Research Society, 41(11), 1073-1076.

Sadler, J. M., Haselden, N., Mellon, K., Hackel, A., Son, V., Mayfield, J., ... & Goodall, J. L. (2017). Impact of sea-level rise on roadway flooding in the Hampton Roads region, Virginia. J. Infrastruct. Syst., 23(4), 05017006. https://doi.org/10.1061/(ASCE)IS.1943-555X.0000397.

Seigel, Rachel, 2021. “Flood Analysis of Bridge-Stream Interactions using Two-Dimensional Models”. Graduate College Dissertations and Theses. 1456. Available from: https://scholarworks.uvm.edu/graddis/1456.

Seo, B. C., Keem, M., Hammond, R., Demir, I., & Krajewski, W. F. (2019). A pilot infrastructure for searching rainfall metadata and generating rainfall product using the big data of NEXRAD. *Environmental modelling & software*, *117*, 69-75.

Shang, K., & Hossen, Z. (2013). Applying fuzzy logic to risk assessment and decision-making. Casualty Actuarial Society, Canadian Institute of Actuaries, Society of Actuaries.

Shariati, M., Kazemi, M., Naderi Samani, R., Kaviani Rad, A., Kazemi Garajeh, M., & Kariminejad, N. (2023). An integrated geospatial and statistical approach for flood hazard assessment. Environmental Earth Sciences, 82(16), 384.

Silverman, B.W. (1986). Density Estimation for Statistics and Data Analysis. London: Chapman & Hall.

Sit, M., Seo, B. C., & Demir, I. (2021). Iowarain: A statewide rain event dataset based on weather radars and quantitative precipitation estimation. arXiv preprint arXiv:2107.03432. https://doi.org/10.48550/arXiv.2107.03432

Tanir, T., Yildirim, E., Ferreira, C. M., & Demir, I. (2024). Social vulnerability and climate risk assessment for agricultural communities in the United States. *Science of The Total Environment*, *908*, 168346.

U.S. Census Bureau. (2017). TIGER/Line Shapefile, 2017, nation, U.S. primary roads, national shapefile. U.S. Department of Commerce. https://catalog.data.gov

U.S. Census Bureau. (2020). 2020 Census Summary File 1 (SF1): Block group population data for Iowa. U.S. Department of Commerce. https://data.census.gov/

U.S. Department of Agriculture, Economic Research Service. (2024). Rural-Urban Continuum Codes and Urban Influence Codes. U.S. Department of Agriculture. https://www.ers.usda.gov/

US DOT (1995). National Bridge Inventory (NBI) – Based on the Coding Guide. Retrieved Online at: https://www.fhwa.dot.gov/bridge/mtguide.cfm

USGS. (2010). Floods of May 30 to June 15, 2008, in the Iowa River and Cedar River Basins, Eastern Iowa. Retrieved from https://pubs.usgs.gov.

Vaidya, O. S., & Kumar, S. (2006). Analytic hierarchy process: An overview of applications. European Journal of Operational Research, 169(1), 1–29

Wang, Y.-M., Liu, J., & Elhag, T. M. S. (2008). An integrated AHP–DEA methodology for bridge risk assessment. Computers & Industrial Engineering, 54(3), 513–525. https://doi.org/10.1016/j.cie.2007.09.002.

Wright, L., Chinowsky, P., Strzepek, K., Jones, R., Streeter, R., Smith, J. B., Mayotte, J.-M., Powell, A., Jantarasami, L., & Perkins, W. (2012). Estimated effects of climate change on flood vulnerability of U.S. bridges. Mitigation and Adaptation Strategies for Global Change, 17(8), 939–955. https://doi.org/10.1007/s11027-011-9354-2

Xu, H., Muste, M., & Demir, I. (2019). Web-based geospatial platform for the analysis and forecasting of sedimentation at culverts. *Journal of Hydroinformatics*, *21*(6), 1064-1081.

Yang, X.-l., Ding, J.-h., & Hou, H. (2013). Application of a triangular fuzzy AHP approach for flood risk evaluation and response measures analysis. Natural Hazards, 68(2), 657–674. https://doi.org/10.1007/s11069-013-0642-x

Yildirim, E., Just, C., & Demir, I. (2022). Flood risk assessment and quantification at the community and property level in the State of Iowa. International journal of disaster risk reduction, 77, 103106.

Yildirim, E., Alabbad, Y., & Demir, I. (2023). Non-structural flood mitigation optimization at community scale: Middle Cedar Case Study. *Journal of environmental management*, *346*, 119025.

Zhang, W., Villarini, G., Vecchi, G.A., Smith, J.A., 2018. Urbanization exacerbated the rainfall and flooding caused by hurricane Harvey in Houston. Nature 563 (7731), 384–388. https://doi.org/10.1038/s41586-018-0676-z.

Ziegelaar, M., & Kuleshov, Y. (2022). Flood Exposure Assessment and Mapping: A Case Study for Australia's Hawkesbury-Nepean Catchment. Hydrology, 9(11), 193.